Available online at www.sciencedirect.com
ScienceDirect
Chinese Journal of Natural Medicines 2023, **21**(2): 83-98
doi: 10.1016/S1875-5364(23)60392-9
Chinese Journal of Natural Medicines

•Original article•

Screening the effective components in treating dampness stagnancy due to spleen deficiency syndrome and elucidating the potential mechanism of Poria water extract

LI Huijun[1], ZHANG Dandan[1], WANG Tianhe[1], LUO Xinyao[1], XIA Heyuan[1], PAN Xiang[1], HAN Sijie[1], YOU Pengtao[1], WEI Qiong[1], LIU Dan[1], ZOU Zhongmei[1, 2*], YE Xiaochuan[1*]

[1] *Hubei Key Laboratory of Resources and Chemistry of Chinese Medicine, School of Pharmacy, Hubei University of Chinese Medicine, Wuhan 430065, China;*
[2] *Institute of Medicinal Plant Development, Chinese Academy of Medical Sciences and Peking Union Medical College, Beijing 100193, China*

Available online 20 Feb., 2023

[ABSTRACT] Poria is an important medicine for inducing diuresis to drain dampness from the middle energizer. However, the specific effective components and the potential mechanism of Poria remain largely unknown. To identify the effective components and the mechanism of Poria water extract (PWE) to treat dampness stagnancy due to spleen deficiency syndrome (DSSD), a rat model of DSSD was established through weight-loaded forced swimming, intragastric ice-water stimulation, humid living environment, and alternate-day fasting for 21 days. After 14 days of treatment with PWE, the results indicated that PWE increased fecal moisture percentage, urine output, D-xylose level and weight; amylase, albumin, and total protein levels; and the swimming time of rats with DSSD to different extents. Eleven highly related components were screened out using the spectrum-effect relationship and LC-MS. Mechanistic studies revealed that PWE significantly increased the expression of serum motilin (MTL), gastrin (GAS), ADCY5/6, p-PKA$\alpha/\beta/\gamma$ cat, and phosphorylated cAMP-response element binding protein in the stomach, and AQP3 expression in the colon. Moreover, it decreased the levels of serum ADH, the expression of AQP3 and AQP4 in the stomach, AQP1 and AQP3 in the duodenum, and AQP4 in the colon. PWE induced diuresis to drain dampness in rats with DSSD. Eleven main effective components were identified in PWE. They exerted therapeutic effect by regulating the AC-cAMP-AQP signaling pathway in the stomach, MTL and GAS levels in the serum, AQP1 and AQP3 expression in the duodenum, and AQP3 and AQP4 expression in the colon.

[KEY WORDS] Poria water extract; Dampness stagnancy due to spleen deficiency syndrome; Spectrum-effect relationship; Effective components; Mechanisms

[CLC Number] R965 **[Document code]** A **[Article ID]** 2095-6975(2023)02-0083-16

Introduction

In the theory of traditional Chinese medicine, the clinical manifestations of dampness stagnancy due to spleen deficiency syndrome (DSSD) include poor appetite, a bitter taste in the mouth, thick and slimy tongue, abdominal fullness, discomfort, dizziness, weak or fatigued limbs, and frequent edema [1]. The occurrence and development of DSSD in humans are closely related to the surroundings and diet. Wet weather, humid living environment, and wading in the rain are factors by which dampness invades the human body from the outside. Tea addiction and improper diet can damage the Yang Qi of the spleen and the stomach, resulting in endogenous dampness. DSSD syndrome has been correlated with the occurrence and development of several diseases such as chronic gastritis [2]. The symptoms of DSSD can adversely affect the quality of life of individuals.

Traditional Chinese medicine maintains a holistic view of the body. The spleen in modern clinical practice refers to the gastrointestinal digestive system and its physiological function. Therefore, proteins closely related to water regulation in the stomach, small intestine, and colon may be associated with the occurrence of DSSD. Several reports suggested that aquaporin (AQP)-3 and AQP4 in the stomach and colon [3]; AQP1 and AQP3 in the small intestine [4, 5]; and the "AC-

[Received on] 12-Sep.-2022
[Research funding] This work was supported by the Key Technologies Research and Development Program (No. 2017YFC1703004) and Hubei Technological Innovation Special Fund (No. 2019ACA121).
[*Corresponding author] E-mails: zmzou@implad.ac.cn (ZOU Zhongmei); Chuan9069@hbtcm.edu.cn (YE Xiaochuan)
These authors have no conflict of interest to declare.

cAMP-AQP" signaling pathway [6] in the stomach are closely related to water metabolism, which may be involved in the occurrence of DSSD. Gastrointestinal hormones can also be used to characterize gastrointestinal function [7].

Traditional Chinese medicines have been used in clinical practice for thousands of years owing to its proven efficacy, wide indications, high safety profile, and low toxicity [8]. Poria, also known as Fuling, is the dried sclerotium of *Poria cocos* (Schw.) Wolf belonging to the family Polyporaceae. It is cultivated in China, Korea, Japan, and North America. The effects of Poria in traditional Chinese medicine include inducing diuresis to drain dampness, invigorating the spleen, and tranquilizing the mind [9]. Poria exerts antitumor [10], antioxidant [11], anti-inflammatory [12], diuretic [13], and immunomodulatory effects [14]. It is used as an important medicine to induce diuresis and drain dampness, which helps treat dampness retention in the upper, middle, and lower energizers. In our previous study, Poria water extract (PWE) improved the condition of damp retention in the lower energizer in rats [15] and promoted diuresis and dampness in rats with damp retention in the upper energizer [16]. The Chinese Pharmacopoeia states that Poria can be used to treat diarrhea due to spleen deficiency (2020 Edition). However, there are no reports concerning the relationship between PWE and DSSD using modern pharmacological experiments. The chemical constituents of Poria have been deeply investigated [17, 18]; however, studies on the components of PWE responsible for inducing diuresis to drain dampness have not yet been reported.

Traditional Chinese medicines contains multiple chemical compounds that exert various effects at multiple channels, multiple levels, and multiple targets. The concept of the spectrum-effect (fingerprint-effect) relationship was proposed in 2002 for the first time [19]. It is usually used to elucidate the pharmacodynamic foundation of the effective components of traditional Chinese medicines and to explore the correlation of fingerprints with pharmacological activity [20]. Additionally, this approach can be used to identify the quality markers of traditional Chinese medicines. Therefore, the spectrum-effect relationship is an important part of traditional Chinese medicine research. Pharmacodynamic assessment and information processing serve as crucial factors for investigating on the spectrum-effect relationship through establishment of fingerprints. Owing to the considerable nonlinearity between the components in the fingerprint chromatogram and the efficacy of traditional Chinese medicines, various methods, such as partial least squares regression (PLSR) analysis and gray relational analysis (GRA) [21], are used to explain these relationships.

In this study, ultra-high performance liquid chromatography (UPLC) was used to establish the chromatographic fingerprints of 10 batches of PWE. The efficacy of draining dampness by induction of diuresis was evaluated based on fecal moisture percentage, urine output, and D-xylose level; weight and swimming time; and amylase (AMS), albumin (ALB), and total protein (TP) levels. Furthermore, GRA and PLSR analysis were used to analyze the spectrum-effect relationship. The effective components were identified by comparing the chromatograms of the 11 reference substances with that of the test sample and by liquid chromatography-mass spectrometry (LC-MS). Moreover, motilin (MTL), gastrin (GAS), and antidiuretic hormone (ADH) levels in the serum; adenylate cyclase (AC; ADCY5/6), protein kinase A (PKA; PKA*α*/*β*/*γ* cat), phosphorylated protein kinase A (p-PKA*α*/*β*/*γ* cat), cAMP-response element binding protein (CREB), phosphorylated CREB (p-CREB), AQP3, and AQP4 expression in the stomach; AQP1 and AQP3 expression in the duodenum; and AQP3 and AQP4 expression in the colon were determined to elucidate the possible mechanism of PWE in treating DSSD.

Materials and Methods

Materials and reagents

Ten batches of Poria were collected from Hubei, Yunnan, Fujian, Henan, Hunan, and Anhui Provinces in China. All samples were identified as the sclerotia of *Poria cocos* (Schw.) Wolf by Prof. YE Xiaochuan from Hubei University of Chinese Medicine (Hubei, China). A voucher specimen was deposited in the herbarium of Hubei Key Laboratory of Resources and Chemistry of Chinese Medicine, Hubei University of Chinese Medicine, Wuhan, China (Supplementary Table 1).

Acetonitrile was purchased from Merck (UPLC, Germany). Pachymic acid (CAS: 29070-92-6), dehydropachymic acid (CAS: 77012-31-8), poricoic acid A (CAS: 137551-38-3), poricoic acid B (CAS: 137551-39-4), polyporenic acid C (CAS: 465-18-9), dehydrotumulosic acid (CAS: 6754-16-1), 16*α*-hydroxydehydrotrametenolic acid (CAS: 176390-66-2), 16*α*-hydroxytrametenolic acid (CAS: 176390-68-4), dehydroeburicoic acid (CAS: 6879-05-6), and 3-*O*-acetyl-16*α*-hydroxydehydrotrametenolic acid (CAS: 168293-14-9) were purchased from Chengdu Push Bio-Technology Co., Ltd. (Chengdu, China). Dehydrotrametenolic acid (CAS: 29220-16-4) was purchased from Shanghai Yuanye Bio-Technology Co., Ltd. (Shanghai, China). The purity of all reference compounds was > 98%. Xiangsha Weiling pill (XWP), as the positive-control drug, was prepared following the method stated in the Chinese Pharmacopoeia (version 2015). All reagents used in the study were of analytical grade.

Preparation of sample solutions

Preparation of PWE

The dried powder of 10 batches of Poria was soaked overnight in ten volumes of water and extracted twice by refluxing at 100 °C for 1 h each time. The aqueous extracts were combined and concentrated to obtain PWE (equivalent to 0.75 g·mL^{-1} of the crude drug). A certain amount of the extract was freeze-dried and the remainder was stored at 4 °C until further use [22]. For UPLC and LC-MS, the extracts were dissolved in methanol (50 mg·mL^{-1}), ultrasonicated for 1 h,

centrifuged at 2504 × *g* for 10 min, volatilized, redissolved in 2 mL methanol, and filtered through a 0.22-μm nylon membrane to obtain the test solution (equivalent to 16 g·mL^{-1} of the crude drug).

Preparation of the reference solution

A mixed stock solution of 11 reference compounds (Fig. 1) was prepared by dissolving each compound in methanol. The final concentrations of pachymic acid, dehydropachymic acid, poricoic acid A, poricoic acid B, polyporenic acid C, dehydrotumulosic acid, 16*α*-hydroxydehydrotrametenolic acid, 16*α*-hydroxytrametenolic acid, dehydroeburicoic acid, 3-*O*-acetyl-16*α*-hydroxydehydrotrametenolic acid, and dehydrotrametenolic acid were 17.44, 15.36, 8.08, 10.56, 3.92, 8.16, 9.12, 8.64, 7.04, 10.4, and 3.84 μg·mL^{-1}, respectively. The solution was stored at 4 °C until use and filtered through a 0.22-μm membrane filter.

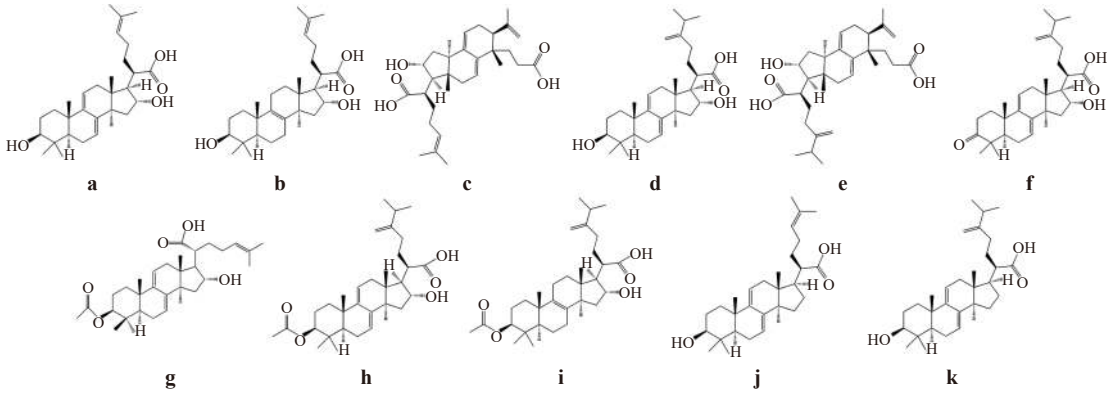

Fig. 1 Structures of the 11 reference substances (a: 16*α*-hydroxydehydrotrametenolic acid, b: 16*α*-hydroxytrametenolic acid, c: poricoic acid B, d: dehydrotumulosic acid, e: poricoic acid A, f: polyporenic acid C, g: 3-*O*-acetyl-16*α*-hydroxydehydrotrametenolic acid, h: dehydropachymic acid, i: pachymic acid, j: dehydrotrametenolic acid, and k: dehydroeburicoic acid)

UPLC-diode array detector (DAD) to acquire fingerprints, and LC-MS

The chromatographic conditions were set as previously described [23]: UPLC was performed on an Agilent 1290 Ultra-Performance Liquid Chromatography unit (Agilent Technologies Co., Ltd., USA) equipped with a vacuum degasser, a quaternionic pump, an auto-sampler, and a DAD controlled using Agilent ChemStation software. Chromatographic separations were performed using a C_{18} chromatographic column (2.1 mm × 100 mm, 1.8 μm, Waters Corp., MA, USA). The mobile phase consisted of solvent A (0.1% aqueous phosphoric acid), solvent B (acetonitrile), and solvent C (methanol). Gradient elution was used, which was programmed as follows: 0–4 min: 55%–85% B and 3% C (flow rate: 0.4–0.2 mL·min^{-1}); 4–8 min: 85%−97% B and 3% C (flow rate: 0.2 mL·min^{-1}); 8–10 min: 97%−100% B and 3%−0% C (flow rate: 0.2–0.4 mL·min^{-1}); and 10–15 min: 100% B (flow rate: 0.4 mL·min^{-1}). The column was conditioned at 40 °C, the detection wavelengths were set at 210 and 242 nm, and the injection volume was 2 μL.

An ACQUITY UPLC−G2 QTOF™ system (Waters Technologies, Manchester, United Kingdom) with an electrospray ionization source (ESI) was used for MS and operated in the negative ion mode. The capillary voltage was 2.5 kV (−) and the sample cone voltage was 30 V. Nitrogen was selected as the drying gas, the flow rate of the desolvation gas was 500 L·h^{-1} at 500 °C, and the cone gas rate was set to 50 L·h^{-1} with the source temperature at 100 °C. Data were collected in the centroid mode from *m/z* 100 to 1000, with a scan time of 0.2 s and an interscan delay of 0.02 s over the analysis period.

Animal experiments

Experimental animals

Male Wistar rats weighing 160−200 g were housed in a sterile-pathogen-free-level laboratory. The room temperature was controlled at 18−25 °C, with a humidity of 50% ± 5%. A 12-h light/dark cycle was implemented, and rats were fed a standard diet, with free access to water. All animal experiments were approved by the Animal Ethics Committee of Hubei University of Chinese Medicine (No: HUCMS 202107003).

Pharmacodynamics of different doses of PWE on rats with DSSD

After acclimatization for seven days, the rats were randomly divided into six groups (n = 10): a control group, a model group, a XWP (positive drug) group [24], a low-dose PWE (LPWE) group, a medium-dose PWE (MPWE) group, and a high-dose PWE (HPWE) group. In addition to the control group, the other groups were subjected to weight-bearing swimming for 15 min and then administered with cold water (4 °C; 2 mL/100 g body weight) daily. Rats in groups other than the control group were housed in cages with wet padding (padding : water, 1 : 5), fasted, and fed sufficient food on alternate days throughout the modeling process. Meanwhile, rats in the control group were fed a standard diet and housed in standard conditions [25]. Twenty-one days after modeling, rats in the XWP, LPWE, MPWE, and HPWE groups were orally administered with the indicated drugs (1.73, 1.5, 7.5, and 15 g·kg^{-1}, respectively), once daily for consecutive 14 days at a volume corresponding to that of normal saline administered to rats in the control and model groups. On the 13th day of administration, the rats were made

to swim with a load of lead rings weighing approximately 10% of their body weight attached to their tail. The swimming time was measured from the beginning until the point at which they could not return to the surface of the water 8 s after sinking. Then, the rats were helped out of the tank and returned to their cages for recovery. After the last administration of the drugs, the rats were housed individually in metabolic cages and fasted, with free access to water. Urine samples were collected within 12 h. D-xylose solution (3%; 2 mL/100 g body weight) was intragastrically administered to rats. Exactly 1 h later, all experimental animals were anesthetized with pentobarbital, subjected to 12-h preoperative fasting, and provided drinking water *ad libitum*. Blood samples were collected from the abdominal aorta using vacuum blood-collection tubes. Tissue samples were immediately obtained from the stomach, duodenum, and colon after serum collection.

Pharmacodynamic studies on the 10 batches of PWE on rats with DSSD

After acclimatization for seven days, rats were randomly divided into the following 13 groups (n = 10): a control group, a model group, a XWP group, and S1−S10 PWE (S1−S10) groups. The modeling methods for all groups except the control group were similar to the pharmacological experiments using PWE at different doses. Twenty-one days after modeling, rats in the XWP and S1−S10 groups were gavaged with the indicated drugs (1.73 and 7.5 $g \cdot kg^{-1}$, respectively) once daily for consecutive 14 days. The serum and tissues of the stomach, duodenum, and colon were collected.

General conditions of rats with DSSD

The hair, feces, and urine of rats, and the changes in their mental and active state were observed. Their body weights were recorded daily during the study.

Measurement of serum indices

Serum D-xylose, ALB, and TP levels were determined by the corresponding assay kits (Nanjing Jiancheng Bioengineering Institute, Nanjing, China). Serum AMS, MTL, GAS, and ADH levels were detected using commercially available enzyme-linked immunosorbent assay (ELISA) kits (Shanghai Fusheng Industrial Co., Ltd., Shanghai, China), according to the manufacturer's instructions.

Hematoxylin-eosin (H&E) staining

Stomach tissue samples were fixed with 10% formaldehyde for more than 24 h and then washed with water to remove formaldehyde. Next, the samples were dehydrated with ethanol, cleared in xylene, embedded in paraffin, sectioned at 4-μm thickness, stained with H&E, and observed under a microscope (DS-U3; Nikon, Tokyo, Japan).

Immunohistochemistry

The stomach, duodenum, and colon tissues collected from the sacrificed rats were embedded in paraffin, sectioned (4 μm), dewaxed with xylene, and hydrated with gradient alcohol. Then, microwave repair was conducted using 0.01 $mol \cdot L^{-1}$ sodium citrate buffer (pH 6.0, 15 min) and endogenous peroxidase was inactivated by blocking the sections with 3% H_2O_2 for 25 min. Next, the sections were blocked with 3% bovine serum albumin for 30 min and incubated with primary anti-AQP3 antibody (1 : 1000; GB11395, Servicebio) and anti-AQP4 antibody (1 : 12 000; GB11529, Servicebio) at 4 °C overnight. Goat anti-rabbit IgG (1 : 200, G1213-100UL, Servicebio) was added and incubated at room temperature for 50 min. After the sections were cleared with phosphate-buffered saline, 3,3′-diaminobenzidine was used for color development and the sections were observed under a microscope (DS-U3; Nikon, Tokyo, Japan).

Western blot

The stomach, duodenum, and colon tissues were ground in liquid nitrogen, lysed with RIPA lysis buffer (containing 1% phenylmethylsulfonyl fluoride), and centrifuged at 805 × g (at 4 °C for 5 min) to extract the total protein. Proteins were quantified using a protein assay kit (ASPEN Biotechnology Co., Ltd., Wuhan, China). The protein sample was boiled for 5 min, cooled on ice, and centrifuged for 30 s; the supernatant was collected for polyacrylamide gel electrophoresis. Next, the proteins were transferred to polyvinylidene fluoride membranes and electrophoresed at 300 mA for 90 min. Then, the membranes were blocked with 5% skimmed milk at room temperature for 1 h and incubated with primary anti-ADCY5/6 antibody (1 : 10 000; df3508, Affinity, USA), anti-PKA$\alpha/\beta/\gamma$ cat antibody (1 : 1000; abp52222, Abbkine, China), anti-p-PKA$\alpha/\beta/\gamma$ cat antibody (1 : 500; abp55741, Abbkine, China), anti-CREB antibody (1 : 1000; abp51045, Abbkine, China), anti-p-CREB antibody (1 : 500; abp50507, Abbkine, China), anti-AQP1 antibody (1 : 10 000; 20333-1-AP, Proteintech, China), anti-AQP3 antibody (1 : 1000; bs-1253R, BIOSS, China), and anti-AQP4 antibody (1 : 1000; bs-0634R, BIOSS, China) at 4 °C overnight. The membranes were then rinsed with TBST three times and incubated with luciferin-labeled goat anti-rabbit secondary antibodies (1 : 10 000; AS1107, ASPEN, China) at room temperature for 30 min and washed four times. Finally, the membranes were treated with enhanced chemiluminescence chromogenic agent and imaged using a membrane scanner (LiDE110; Canon, Japan).

Statistical analysis

All data are expressed as the mean ± SD (n = 10). Differences among groups were analyzed using Student's t-test analysis of variance. Statistical analyses were performed using IBM SPSS V.25.0 (SPSS Inc., Chicago, USA). $P < 0.05$ was considered to be statistically significant.

Spectrum-effect relationship analysis

To identify the active components, we first used the pharmacodynamic indices as the reference series and the 21 common peaks as the comparison series. Then, PLSR analysis and GRA were used to establish the correlation between the ingredients of PWE and its therapeutic effect on DSSD. The larger the absolute value of the PLSR coeffcient, the greater the contribution of the peak to efficacy. A positive value indicated a positive correlation with drug effect, whereas a negative value indicated a negative correlation. Thus,

compounds with positive values were identified as the active ingredients of PWE in this study. The gray relational coefficients (R) for each common peak were obtained and peaks with $R > 0.6$ were identified as the effective ingredients of PWE.

Results

UPLC fingerprints and LC-MS

The Chinese Medicine Chromatographic Fingerprint Similarity Evaluation System (version 2012 A) was used to obtain the chromatogram of S1 as the reference spectrum. Chromatographic peaks were calibrated using the multipoint method, and the median method was used to generate the control chromatogram. Twenty-one characteristic peaks were screened out from the spectra of 10 batches of PWE and numbered P1−P21 (Figs. 2A and 2B). Eleven peaks were identified by comparison with the chromatograms of the reference substances (Fig. 2C). The similarity of the 10 batches of PWE ranged from 0.772 to 0.997, which indicated that these batches could be used for spectrum-effect analysis.

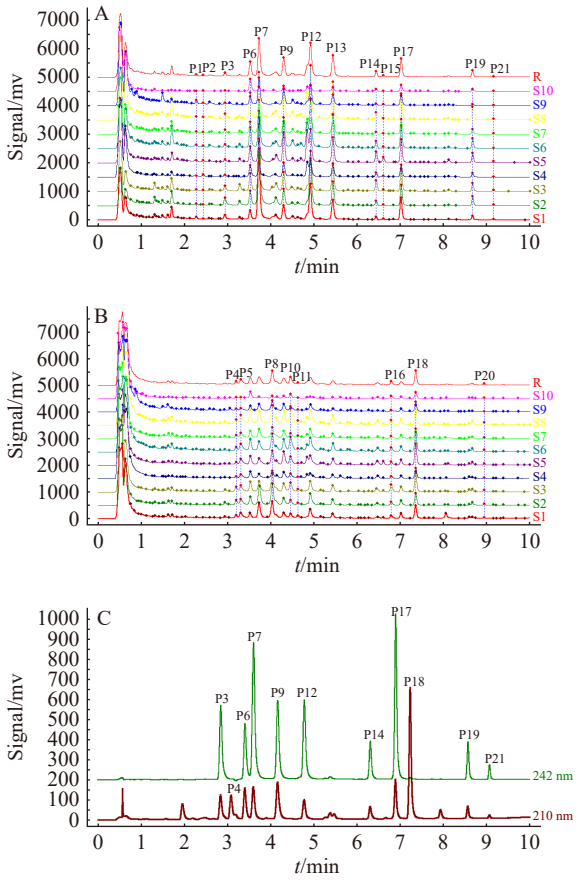

Fig. 2 Matching chromatograms of the 10 batches of PWE characterized by UPLC (A: 242 nm; B: 210 nm). Chromatograms of the 11 reference substances (C). P3: 16*α*-hydroxydehydrotrametenolic acid, P4: 16*α*-hydroxytrametenolic acid, P6: poricoic acid B, P7: dehydrotumulosic acid, P9: poricoic acid A, P12: polyporenic acid C, P14: 3-*O*-acetyl-16*α*-hydroxydehydrotrametenolic acid, P17: dehydropachymic acid, P18: pachymic acid, P19: dehydrotrametenolic acid, P21: dehydroeburicoic acid

UPLC-MS was used to qualitatively assign the characteristic peaks of the PWE fingerprint, and the negative ion mode of ESI was used. Peak identification and assignment of UPLC fingerprint were based on the comparison of their retention time (t_R) and MS ion data with the reference compounds and the literature [26]. The MS data of 21 compounds (peaks) in PWE are shown in Fig. 3 and Table 1.

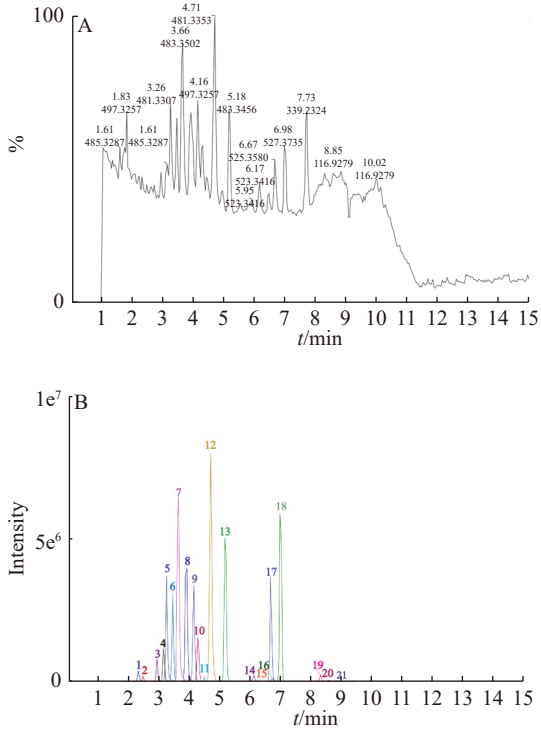

Fig. 3 Total ion chromatogram of PWE in the negative ion mode by UPLC-QTOF-MS/MS (A) and extracted ion chromatograms of 21 triterpenes in PWE by UPLC-QTOF-MS/MS (B)

Therapeutic effects of PWE in treating DSSD

The therapeutic effect of PWE was evaluated based on changes in body parameters and biochemical indices. Before experiments, all rats were active; their fur was smooth, white, and clean; and their feces and urine were normal. During the study, rats in the control group exhibited no obvious abnormalities and there was a gradual increase in their weights. Twenty-one days after modeling, the rats showed typical symptoms of DSSD, such as withered hair, lethargy, and grouping together. The weights of the model rats did not increase compared with those in the control group, and the fecal moisture percentage, urine output, D-xylose level, and swimming time were significantly lower in the model rats compared with those in the control group ($P < 0.01$, $P < 0.05$). The results are presented in Figs. 4A−4E.

Pharmacological study using different doses of PWE

The symptoms of DSSD in rats significantly improved

Table 1 MS data of 21 compounds (peaks) in PWE

Peak No.	t_R/min	Identification	Chemical formula	Calculated $[M-H]^-$ (*m/z*)	Observe $[M-H]^-$ (*m/z*)	Error ($\times 10^{-6}$)	MS/MS
1	2.33	3,24-Dioxo-16*α*-hydroxylanosta-7,9(11)-dien-21-oic acid	$C_{30}H_{44}O_5$	483.3110	483.3096	−2.90	385.2356, 367.2271, 387.2520, 369.2391, 85.0648, 325.2170, 353.2122, 323.1596
2	2.49	25-Hydroxyporicoic acid C	$C_{31}H_{46}O_5$	497.3267	497.3257	−2.01	467.3177, 407.2958, 423.3208, 421.3092, 253.1587, 321.2187, 373.2559, 339.2285, 481.3263
3*	2.95	16*α*-Hydroxy dehydrotrametenolic acid	$C_{30}H_{46}O_4$	469.3318	469.3297	−4.47	407.2917, 423.3292, 375.2685, 337.2513, 393.2758, 391.2964, 313.2130, 311.2011
4*	3.16	16*α*-Hydroxytrametenolic acid	$C_{30}H_{48}O_4$	471.3474	471.3460	−2.97	409.3111, 407.2917, 423.3250, 207.1727, 427.3203, 425.3372, 275.2020
5#	3.26	Polyporenic acid C	$C_{31}H_{46}O_4$	481.3318	481.3307	−2.29	466.3089, 421.3092, 403.3009, 405.2773, 383.2526, 255.1371, 259.1698
6*	3.47	Poricoic acid B	$C_{30}H_{44}O_5$	483.311	483.3096	−2.90	409.2738, 211.1473, 421.3092, 365.2832, 437.3393, 349.2515
7*	3.66	Dehydrotumulosic acid	$C_{31}H_{48}O_4$	483.3474	483.3502	5.79	437.3393, 421.3092, 313.2166
8	3.93	Tumulosic acid	$C_{31}H_{50}O_4$	485.3631	485.3647	3.30	423.3250, 221.1879, 275.1986, 441.3742, 339.2701, 355.2627, 371.2566
9*	4.16	Poricoic acid A	$C_{31}H_{46}O_5$	497.3267	497.3257	−2.01	423.2913, 381.3187, 379.2979, 211.1473, 297.2255, 363.2664, 279.2116, 213.1278
10	4.28	Poriacosone B	$C_{30}H_{46}O_5$	485.3267	485.3287	4.12	441.3355, 397.2740, 351.2674, 353.2469, 371.2566, 409.2738, 467.3133
11	4.50	Poricoic acid HE	$C_{32}H_{48}O_6$	527.3373	527.3359	−2.65	431.2791, 413.2690, 397.2372, 83.0502, 369.2430, 469.3297, 371.2566, 97.0650
12*	4.73	Polyporenic acid C	$C_{31}H_{46}O_4$	481.3318	481.3307	−2.29	435.3245, 421.3092, 97.0650, 311.2011, 405.2773, 403.3009, 387.2681, 271.1674
13	5.18	3-*epi*-Dehydrotumulosic acid	$C_{31}H_{48}O_4$	483.3474	483.3456	−3.72	421.3092, 437.3478, 407.2917,405.3145, 389.2857, 273.1911
14*	5.95	3-*O*-Acetyl-16*α*-hydroxy dehydrotrametenolic acid	$C_{32}H_{48}O_5$	511.3423	511.3430	1.37	451.3207, 449.3043, 465.3321, 463.3199, 433.2717, 355.2280, 405.3145
15	6.30	3*β*-*p*-Hydroxy benzoyldehydrotumulosic acid	$C_{38}H_{52}O_6$	603.3686	603.3698	1.99	559.3774, 475.2845, 137.0229, 457.2743, 93.0343
16	6.73	3-*O*-Acetyl-16*α*-hydroxytrametenolic acid	$C_{32}H_{50}O_5$	513.358	513.3594	2.73	453.3329, 207.1786, 467.3531, 391.2924
17*	6.67	Dehydropachymic acid	$C_{33}H_{50}O_5$	525.358	525.358	0.00	465.3365, 481.3667, 479.3514, 429.2656, 439.3544, 421.3470
18*	6.98	Pachymic acid	$C_{33}H_{52}O_5$	527.3736	527.3735	−0.19	465.3365, 467.3531, 221.1910, 405.3103, 317.2123, 497.3257
19*	8.31	Dehydrotrametenolic acid	$C_{30}H_{46}O_3$	453.3369	453.3372	0.66	337.2475, 339.2701, 371.2527, 323.2332, 435.3245
20	8.59	Trametenolic acid	$C_{30}H_{48}O_3$	455.3525	455.3539	3.07	339.2625, 373.2796, 425.3034
21*	8.85	Dehydroeburicoic acid	$C_{31}H_{48}O_3$	467.3525	467.3531	1.28	337.2513, 339.2701, 371.2606, 279.2322

*Compounds identified using reference compounds; #Unrecognized isomer

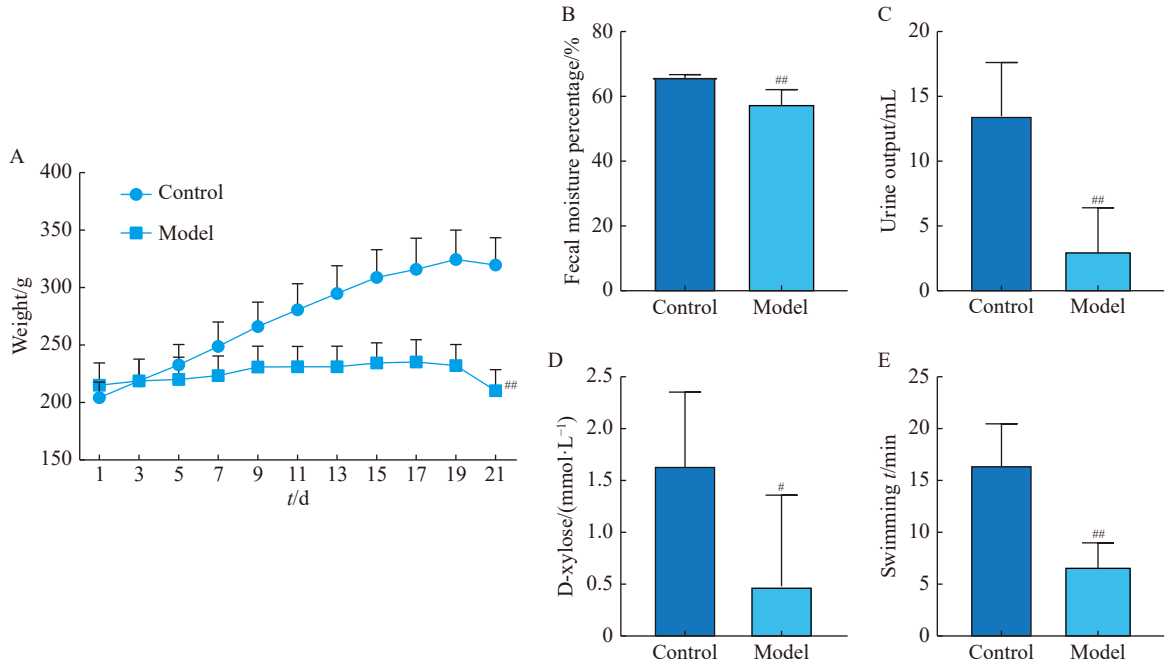

Fig. 4 Changes in weight (A), fecal moisture percentage (B), urine output (C), D-xylose level (D), and swimming time (E) in rats after modeling. Data are expressed as the mean ± SD (n = 10), $^{\#\#}P < 0.01$, $^{\#}P < 0.05$ *vs* the control group

after administration of PWE for 14 days. The fecal moisture percentage, urine output, D-xylose level, weight, AMS and ALB levels, TP, and swimming time of rats in the model group were significantly lower than those in the control group ($P < 0.01$, $P < 0.05$). The urine output, weight, AMS level, and swimming time of rats in the LPWE group were significantly higher compared with those in the model group ($P < 0.01$, $P < 0.05$), whereas the D-xylose level, weight, AMS and ALB levels, TP, and swimming time of rats in the MPWE group were significantly higher compared with those in the model group ($P < 0.01$). The fecal moisture percentage, weight, and swimming time of rats in the HPWE group were significantly higher compared with those in the model group ($P < 0.01$, $P < 0.05$) (Figs. 5A−5H). As shown in Fig. 5I, severe tissue damage was observed in the stomach of the model rats. The structure of the gastric pit disappeared and the fundus glands appeared atrophied to different degrees. For rats in the LPWE, MPWE, and HPWE groups, the gastric fundus glands were arranged tightly and in an orderly manner, and the tissue morphology was restored. The structure of the gastric pit was restored in rats in the MPWE and HPWE groups, but only partially restored in those in the LPWE group.

Pharmacological studies using 10 batches of PWE

After being gavaged with 10 batches of PWE for consecutive 14 days, the rats showed significant improvement in DSSD symptoms. The fecal moisture percentage, urine output, D-xylose level, weight, AMS and ALB levels, TP, and swimming time of rats in the model group were significantly lower than those in the control group ($P < 0.01$, $P < 0.05$). The above-mentioned indicators in rats in the S1−S10 groups increased to different extents compared with those in the model group (Figs. 6A−6H).

Evaluation of total efficacy

The therapeutic effects of traditional Chinese medicines are achieved through multiple targets although DSSD occurs due to the abnormality of several indices in the body. Thus, a single index can not be used to objectively evaluate the overall efficacy. To evaluate the total efficacy of PWE, the weight coefficients were determined using the analytic hierarchy process [15, 27, 28]. The comprehensive score order of total efficacy was calculated considering the weight coefficients. Based on the score table (Supplementary Table 2), the relative importance of each pharmacodynamic index at the same level was compared and a table of priority matrix was constructed for the pairwise comparison of each pharmacodynamic index (Table 2). The weight coefficients of fecal moisture, urine output, D-xylose, body weight, AMS, ALB, TP, and swimming time calculated by the geometric average method were 0.235, 0.235, 0.118, 0.118, 0.118, 0.059, 0.059, and 0.059, respectively. Results from the consistency test showed that the random consistency ratio (CR) was 3.5461×10^{-5}, which was < 0.1, indicating that valid weight coefficients were obtained. Finally, the pharmacodynamics of each pharmacodynamic index was calculated as follows:

$$\text{Single-index pharmacodynamics} = \left[\frac{\text{Drug administration group} - \text{Model group}}{\text{Model group}}\right] \Big/ \left\{\sum_1^n \left[\frac{\text{Drug administration group} - \text{Model group}}{\text{Model group}}\right] / n\right\}.$$

The pharmacodynamics of each pharmacodynamic index of different doses of PWE and the 10 batches of PWE are shown in Tables 3 and 4, respectively.

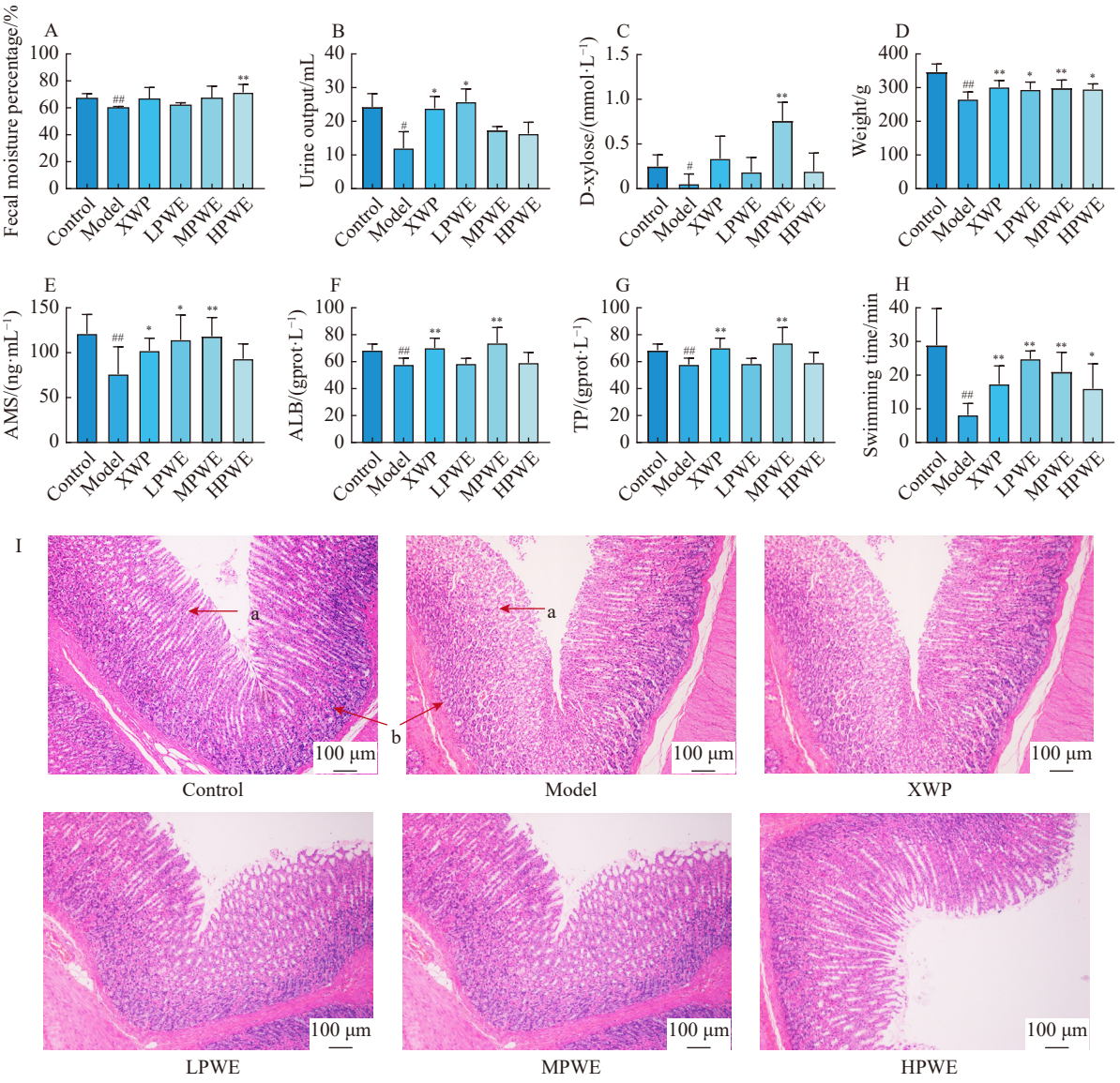

Fig. 5 Effects of different doses of PWE on fecal moisture percentage (A), urine output (B), D-xylose level (C), weight (D), AMS level (E), ALB level (F), TP (G), swimming time (H), and gastric histopathology (I) (a: gastric pit, b: fundus glands; $n = 3$, 100 × magnification). Data are expressed as the mean ± SD ($n = 10$), $^{\#\#}P < 0.01$, $^{\#}P < 0.05$ *vs* the control group; $^{**}P < 0.01$, $^{*}P < 0.05$ *vs* the model group

$$\text{Total efficacy (TE)} = \sum_1^n (\text{Single-index pharmacodynamics} \times \text{weight coefficient of each indicator})$$

where n is the number of efficacy indicators.

The total efficacy (TE) of different doses of PWE was calculated and ranked as follows: MPWE (TE = 1.20) ≈ XWP (TE = 1.12) > LPWE (TE = 0.84) and HPWE (TE = 0.84). Results of the total efficacy of the 10 batches of PWE are shown in Table 5.

Analysis of the spectrum-effect relationship

The peak area of each compound was standardized as follows: $\text{standardized peak area} = [\text{peak area}] / \left[\sum_1^m (\text{peak area})/m\right]$, where m is the number of peaks.

The standardized peak areas of the 10 batches are shown in Supplementary Table 3. GRA and PLSR analysis were conducted to determine the relationship between the standardized peak area and total efficacy data. In GRA (Table 6), the contribution of the peaks of PWE to the pharmacodynamics from high to low was listed as follows: P6 > P17 > P8 > P9 > P16 > P11 > P18 > P5 > P4 > P12 > P7 > P15 > P2 > P13 > P1 > P3 > P10 > P21 > P20 > P14 > P19. The correlation coefficients of all peaks were > 0.6, indicating a correlation with pharmacodynamics. PLSR analysis revealed that 11 compounds were positively correlated with the efficacy of PWE in alleviating DSSD (Fig. 7). The main chemical components found to be positively correlated with efficacy were P3, P4, P5, P7, P8, P11, P13, P14, P16, P17, and P18. Thus, we speculated that 16α-hydroxydehydrotrametenolic acid (P3), 16α-hydroxytrametenolic acid (P4), polyporenic acid C (P5), dehydrotumulosic acid (P7), tumulosic acid (P8),

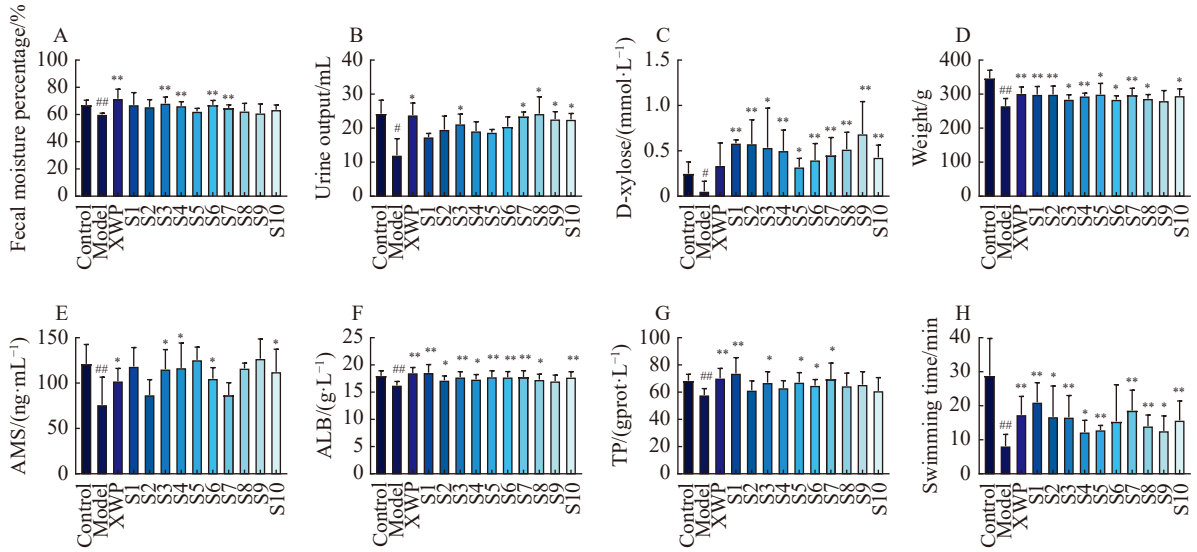

Fig. 6 Effects of the 10 batches of PWE on fecal moisture percentage (A), urine output (B), D-xylose level (C), weight (D), AMS level (E), ALB level (F), TP (G), and swimming time (H). Data are expressed as the mean ± SD (n = 10), $^{\#\#}P < 0.01$, $^{\#}P < 0.05$ *vs* the control group; $^{**}P < 0.01$, $^{*}P < 0.05$ *vs* the model group

Table 2 Priority matrix for the pairwise comparison of targets

Target	Fecal moisture	Urine output	D-xylose	Weight	AMS	ALB	TP	Swimming time
Fecal moisture	1	1	2	2	2	4	4	4
Urine output	1	1	2	2	2	4	4	4
D-xylose	0.5	0.5	1	1	1	2	2	2
Weight	0.5	0.5	1	1	1	2	2	2
AMS	0.5	0.5	1	1	1	2	2	2
ALB	0.25	0.25	0.5	0.5	0.5	1	1	1
TP	0.25	0.25	0.5	0.5	0.5	1	1	1
Swimming time	0.25	0.25	0.5	0.5	0.5	1	1	1

Table 3 Pharmacodynamics of each pharmacodynamic index of different doses of PWE

Group	Fecal moisture	Urine output	D-xylose	Weight	AMS	ALB	TP	Swimming time
XWP	0.97	1.34	1.05	1.12	0.84	1.36	1.63	0.79
LPWE	0.28	1.56	0.51	0.90	1.24	0.12	0.09	1.43
MPWE	1.06	0.61	1.93	1.04	1.37	1.87	2.09	1.10
HPWE	1.69	0.49	0.51	0.94	0.55	0.64	0.18	0.68

poricoic acid HE (P11), 3-*epi*-dehydrotumulosic acid (P13), 3-*O*-acetyl-16*α*-hydroxydehydrotrametenolic acid (P14), 3-*O*-acetyl-16*α*-hydroxytrametenolic acid (P16), dehydropachymic acid (P17), and pachymic acid (P18) were the active components of PWE that play a role in the treatment of DSSD.

Mechanism of PWE in the treatment of DSSD

Effect on serum MTL and GAS levels

MTL and GAS levels in the serum of rats in the model group were significantly lower compared with those in the control group ($P < 0.01$). Serum MTL levels of rats in the LPWE, MPWE, and HPWE groups were significantly higher than those in the model group ($P < 0.01$, Fig. 8A). Serum GAS levels of rats in the MPWE group were significantly higher than that in the model group ($P < 0.01$, Fig. 8B). An upward trend was observed in rats in the LPWE and HPWE groups compared with those in the model group; however, the difference was not significant.

Effect on the "AC-cAMP-AQP" signaling pathway

Results from ELISA showed that ADH levels significantly increased in the model group compared with the control group, and decreased in the MPWE and HPWE groups compared with the model group ($P < 0.01$) (Fig. 9A).

Table 4 Pharmacodynamics of each pharmacodynamic index of the 10 batches of PWE

Group	Fecal moisture	Urine output	D-xylose	Weight	AMS	ALB	TP	Swimming time
XWP	1.68	1.29	0.66	1.31	0.76	1.19	1.48	1.21
S1	1.84	0.58	1.21	1.22	1.24	1.63	1.90	1.69
S2	0.50	0.82	1.21	1.23	0.32	0.66	0.42	1.13
S3	2.11	1.00	1.12	0.69	1.15	1.07	1.09	1.12
S4	0.52	0.78	1.03	1.05	1.19	0.79	0.64	0.54
S5	0.37	0.73	0.62	1.24	1.45	1.11	1.12	0.62
S6	1.28	0.92	0.80	0.69	0.85	1.07	0.84	0.95
S7	1.24	1.25	0.92	1.17	0.31	1.11	1.42	1.38
S8	0.03	1.33	1.08	0.78	1.18	0.75	0.80	0.77
S9	1.03	1.16	1.47	0.56	1.49	0.55	0.93	0.59
S10	0.39	1.15	0.87	1.08	1.06	1.06	0.37	0.99

Table 5 Total efficacy of the 10 batches

Group	Total efficacy	Group	Total efficacy
S1	1.25	S6	0.96
S2	0.77	S7	1.10
S3	1.27	S8	0.81
S4	0.80	S9	1.05
S5	0.82	S10	0.86

Table 6 Gray relationship grade and their order between the 21 peaks and induction of diuresis to obtain the drain dampness effect of PWE

Order	Gray relation grade	Peak number	Order	Gray relation grade	Peak number
1	0.86	6	12	0.80	15
2	0.84	17	13	0.80	2
3	0.83	8	14	0.79	13
4	0.83	9	15	0.79	1
5	0.83	16	16	0.79	3
6	0.82	11	17	0.78	10
7	0.82	18	18	0.78	21
8	0.82	5	19	0.76	20
9	0.81	4	20	0.75	14
10	0.81	12	21	0.74	19
11	0.81	7			

Western blot results showed that the expression of gastric ADCY5/6, p-PKA$\alpha/\beta/\gamma$ cat, and p-CREB remarkably decreased ($P < 0.01$). The expression of ADCY5/6, p-PKA$\alpha/\beta/\gamma$ cat, and p-CREB in the MPWE and HPWE groups was significantly elevated compared with those in the model group ($P < 0.01$). In the LPWE group, only p-PKA$\alpha/\beta/\gamma$ cat expression in gastric tissues significantly increased ($P < 0.05$) (Figs. 9B-a and 9B-b). Results from Western blot and immunohistochemistry showed that the levels of AQP3 and AQP4 in the model group were significantly higher than that in the control group ($P < 0.01$), whereas the levels of AQP3 and AQP4 were significantly reduced in the gastric tissues of rats in the LPWE, MPWE, and HPWE groups ($P < 0.01$, $P < 0.05$) (Figs. 9B−9D). There were no significant differences in PKA$\alpha/\beta/\gamma$ cat and CREB levels among the control, model, and PWE treatment groups, indicating that the disease did not affect PKA$\alpha/\beta/\gamma$ cat and CREB expression.

Expression of AQP1 and AQP3 in the duodenum and AQP3 and AQP4 in the colon

AQP1 and AQP3 expression in the duodenum and AQP4 expression in the colon significantly increased, but AQP3 expression in the colon remarkably decreased in the model group compared with that in the control group ($P < 0.01$). However, in the LPWE, MPWE, and HPWE groups, the expression of AQP1 and AQP3 in the duodenum and AQP4 expression in the colon were significantly declined, whereas AQP3 expression in the colon was obviously elevated compared with that in the model group ($P < 0.05$, $P < 0.01$) (Fig. 10).

Discussion

According to the theory of traditional Chinese medicine, the spleen governs dampness. The occurrence and development of DSSD in humans are closely related to their surroundings and diet. Based on the medicinal properties of Poria, our previous research and preliminary experiments, a modeling method was established to improve the methods reported in the literature [24]. In this study, weight-loading swimming, intragastric ice-water stimulation, and irregular diet were conducted to cause endogenous dampness, whereas living in wet padding was used to make exogenous dampness to establish a more accurate rat model of DSSD. Spleen deficiency was simulated by simultaneously making exogenous

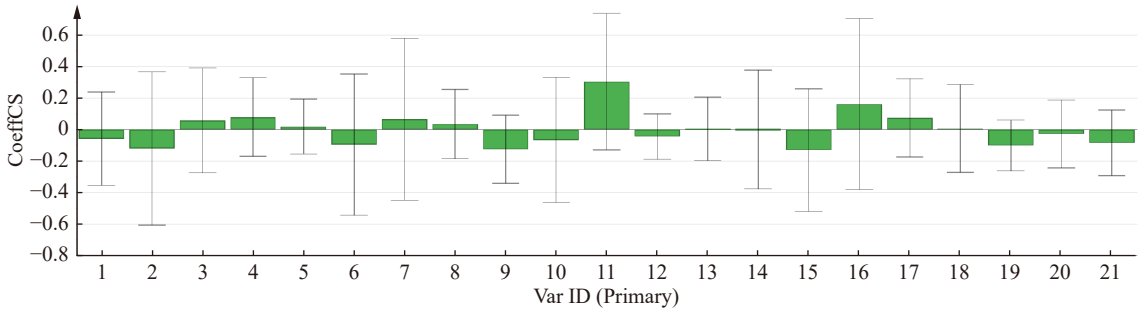

Fig. 7 PLSR analysis of the 21 peaks and induction of diuresis to obtain the drain dampness effect of PWE (VIP plot)

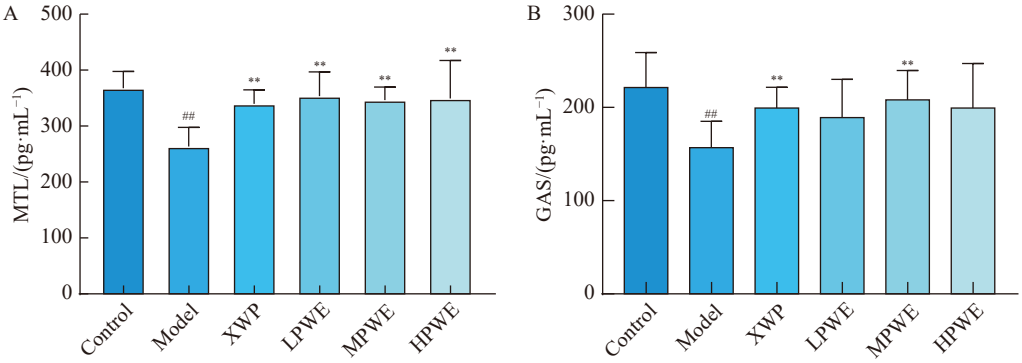

Fig. 8 Effect on MTL (A) and GAS levels (B). Data are expressed as the mean ± SD (n = 10), $^{\#\#}P < 0.01$, $^{\#}P < 0.05$ *vs* the control group; $^{**}P < 0.01$, $^{*}P < 0.05$ *vs* the model group

and endogenous dampness to represent a comprehensive model of DSSD.

Spleen is the hub of water metabolism. In this study, an obvious decrease in fecal moisture percentage was observed in rats with DSSD. Dampness bothers the spleen and water gathers in the intestines during spleen deficiency, resulting in loose stools and diarrhea [29]. Spleen deficiency can also result in Qi deficiency, leading to difficulty to defecate and slowing intestinal peristalsis [30]. We found that model rats had loose stools in the early stage of spleen deficiency. With an extension in modeling time, the symptoms of spleen deficiency were worsened and the stool gradually became more dry. The fecal moisture percentage in the model rats decreased compared with that of control rats at the end of modeling. Although Poria is mainly used to treat loose stools and diarrhea, it is also often used as a principal drug in many traditional Chinese medicine prescriptions to treat spleen-deficiency constipation, indicating its ability to rapidly digest food in the intestines by regulating gastrointestinal function and reducing the reabsorption of water in the intestines [31, 32]. The fecal moisture percentage of rats in the PWE groups increased compared with that in model rats, indicating that PWE intervention may alleviate the symptoms of dry stools by regulating the state of spleen deficiency. The activity of AMS and the D-xylose concentration in the serum were used as markers to reflect digestion and nutrient absorption in rats [33, 34]. The D-xylose and AMS levels of rats in the model group were significantly lower than those in the control group ($P < 0.01$, $P < 0.05$). PWE increased D-xylose and AMS levels, indicating that it improved gastrointestinal absorption function in rats with DSSD to induce diuresis and drain dampness. In a clinical setting, a decrease in TP is commonly seen in water-sodium retention. A decrease in serum ALB levels can cause water in the blood to move to tissues and result in edema [35]. In this study, rats in the model group exhibited decreases in TP and ALB levels compared with those in the control group, whereas each treatment group exhibited increases in TP and ALB levels, indicating that PWE played a role in the treatment of DSSD by regulating the osmotic pressure of plasma colloids.

The spectrum-effect relationship has been successfully used to screen active ingredients in natural products [20]. Compared with other research methods, the spectrum-effect relationship has outstanding advantages as it increases the amount of research to determine the correlation between fingerprints and pharmacological effects. In this study, PLSR analysis and GRA were used to analyze the correlation between the 21 common chromatographic peaks of PWE and its efficacy in treating DSSD. Eleven compounds (16*α*-hydroxydehydrotrametenolic acid, 16*α*-hydroxytrametenolic acid, polyporenic acid C, dehydrotumulosic acid, tumulosic acid, poricoic acid HE, 3-*epi*-dehydrotumulosic acid, 3-*O*-acetyl-16*α*-hydroxydehydrotrametenolic acid, 3-*O*-acetyl-16*α*-hydroxytrametenolic acid, dehydropachymic acid, and pachymic acid) were identified as being closely related to treating DSSD. Network pharmacological analysis revealed that

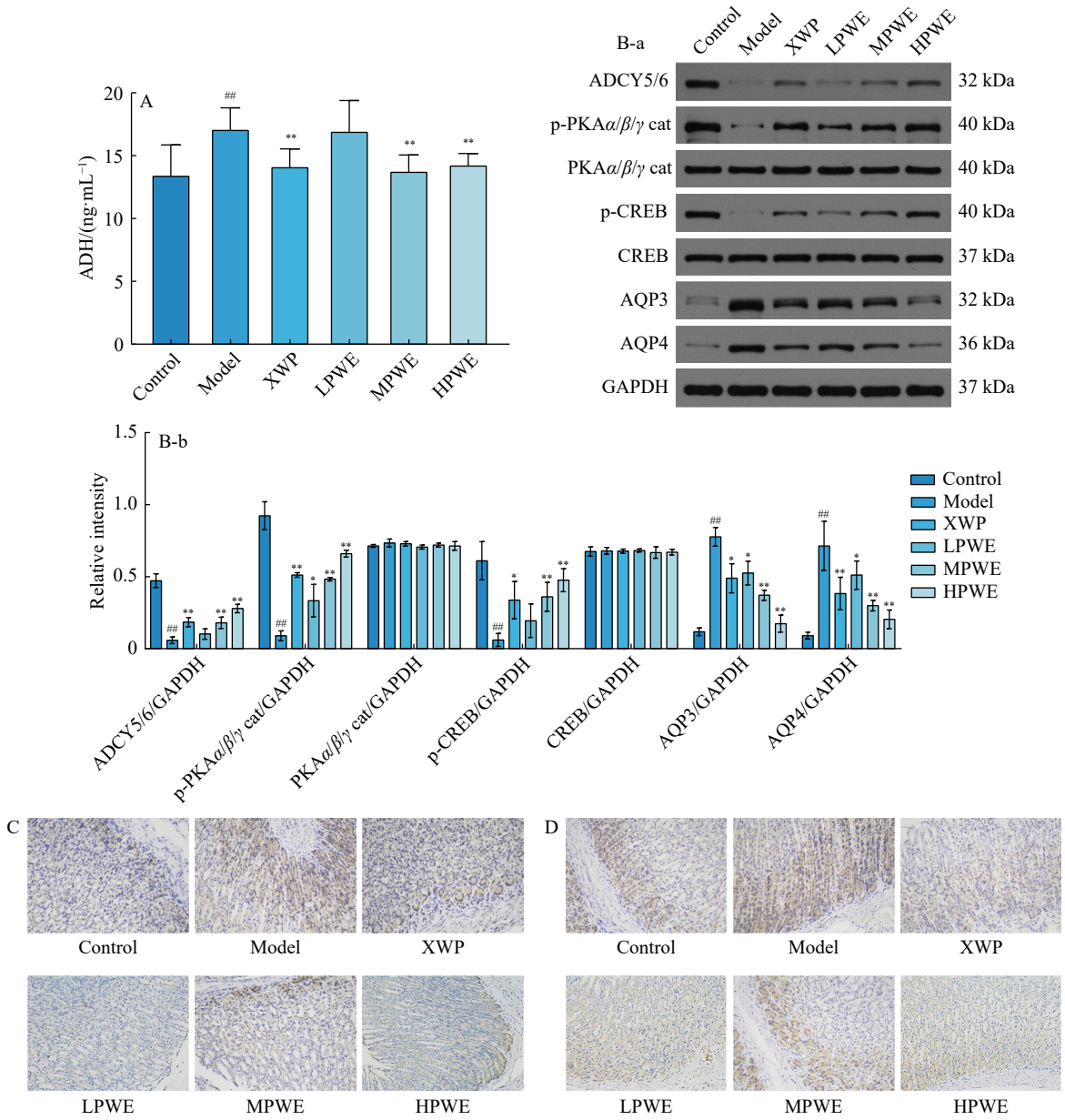

Fig. 9 Effect on the "AC-cAMP-AQP" signaling pathway. (A) ADH; (B) Levels of ADCY5/6, p-PKA*α*/*β*/*γ* cat, PKA*α*/*β*/*γ* cat, p-CREB, CREB, AQP3, and AQP4 by Western blot; (C) Immunohistochemical analysis of AQP3, 200 × magnification; (D) Immunohistochemical analysis of AQP4, 200 × magnification. Data are expressed as the mean ± SD (A: *n* = 10, B–D: *n* = 3), $^{\#\#}P < 0.01$, $^{\#}P < 0.05$ *vs* the control group; $^{**}P < 0.01$, $^{*}P < 0.05$ *vs* the model group

16*α*-hydroxydehydrotrametenolic acid has high biological activity and can be used as a marker to determine the quality of Poria [36]. 16*α*-Hydroxytrametenolic acid can improve intestinal barrier function [37], whereas polyporenic acid C, 3-*epi*-dehydrotumulosic acid, 3-*O*-acetyl-16*α*-hydroxytrametenolic acid, dehydropachymic acid, and pachymic acid show cytotoxicity against two human cancer cell lines [38]. Dehydrotumulosic acid has antihyperglycemic effect [39], whereas tumulosic acid exerts potent inhibitory effect on the tumor promoter 12-*O*-tetradecanoylphorbol-13-acetate–induced early antigen activation in Epstein–Barr virus infections [40]. 3-*O*-acetyl-16*α*-hydroxydehydrotrametenolic acid exhibits anti-inhibitory activity [41]. Although poricoic acid HE was first reported in 2019 [42], no literature has reported its activity. Our results lay a theoretical foundation for further investigating poricoic acid HE. Our study has some drawbacks. This research was not adequate to comprehensively study the effective components of PWE in treating DSSD using the spectrum-effect relationship. We will further verify these effective components using suitable knock-out and knock-in models.

In the Yellow Emperor's Canon of Internal Medicine, dampness and swelling have been reported to belong to the spleen. Spleen deficiency is a fundamental factor that results in DSSD. Spleen deficiency is a complicated pathological

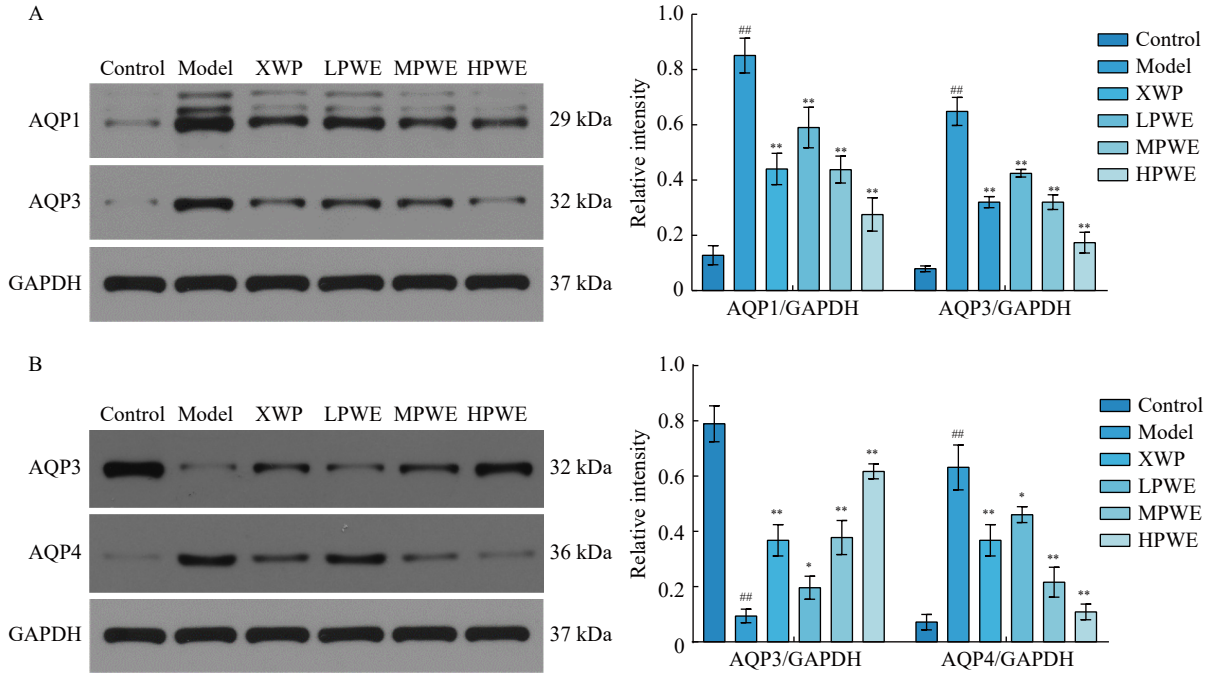

Fig. 10 AQP1 and AQP3 expression in the duodenum (A) and AQP3 and AQP4 expression in the colon (B). Data are expressed as the mean ± SD (n = 3), $^{\#\#}P < 0.01$, $^{\#}P < 0.05$ *vs* the control group; $^{**}P < 0.01$, $^{*}P < 0.05$ *vs* the model group

condition related to an imbalance in gastrointestinal function, resulting in the inhibition of MTL/GAS secretion [43]. As expected, in our study, compared with the control group, MTL and GAS levels in the model group decreased, indicating that rats with DSSD were in a state of spleen deficiency. MTL and GAS levels increased after PWE intervention, which indicated that PWE improved the spleen deficiency of rats with DSSD. The gastrointestinal tract is a major organ for water transport that is only secondary to the kidneys [44]. The AC-cAMP signaling system is the perfect post-receptor signal transduction system. When a ligand (hormones or neurotransmitters) binds to a specific receptor on the cell membrane, G-protein coupled receptors activate AC to catalyze the hydrolysis of ATP to form cAMP, which acts as a second messenger. cAMP further activates PKA, which phosphorylates and regulates various target proteins. When the 133rd serine of the cAMP response element–binding protein (CREB) is phosphorylated and activated [45], treatment of DSSD is mainly achieved by regulating the key target genes that maintain and regulate water metabolism [46]. AQPs are ubiquitously present in the digestive tract of mammals, including the salivary glands, esophagus, stomach, small and large intestines, gallbladder, bile duct, and pancreas [47]. Water is secreted as digestive juices and absorbed by the gastrointestinal epithelia, which can be classified as leaky (small intestine), moderately tight (gastric antrum and colon), and tight (gastric fundus) epithelia [48]. AQP3 and AQP4 are highly expressed in the stomach [47]. The transport, gating, and redistribution of AQPs are mediated by the AC-cAMP signaling pathway [6]. The AC-cAMP signaling pathway can regulate AQPs by the short-term regulation of PKA and long-term regulation of CREB [49]. In this study, we found that PWE upregulated the expression of ADCY5/6, p-PKA, and p-CREB in the stomach; downregulated ADH levels in the serum; and downregulated the expression of AQP3 and AQP4 in the stomach to different extents in rats with DSSD. These targets in the "AC-cAMP-AQP" signaling pathway (Fig. 11) in the stomach may be involved in the mechanism of PWE in treating DSSD. AQP1 and AQP3 are abundantly expressed in the small intestine, whereas AQP3 and AQP4 are the predominant isoforms in the colon [47]. AQP3 is most abundantly expressed in the mucosal epithelial cells of the gastrointestinal tract. When AQP3 expression is reduced in the gastrointestinal tract, the resulting increases in cell-membrane fluidity lead to increases in water reabsorption [50]. Furthermore, we found that PWE reduced the expression of AQP3 in the stomach and duodenum of rats with DSSD ($P < 0.05$, $P < 0.01$). These findings suggested that PWE enhanced water reabsorption in the stomach and duodenum and expelled from the body. However, AQP3 plays a different role in the colon. The transfer of large quantities of water from blood vessels into the intestinal tract is a result of the increase in AQP3 expression [51]. PWE treatment increased AQP3 expression in the colon of rats with DSSD in our study ($P < 0.05$, $P < 0.01$), which was consistent with published data. Moreover, we found that treatment with PWE significantly decreased AQP1 expression in the duodenum and AQP4 expression in the colon ($P < 0.05$, $P < 0.01$). Water in rats with DSSD was further drained out of the body. The spleen has a preference for dryness and not dampness. Dampness is expelled from the body through the regulatory

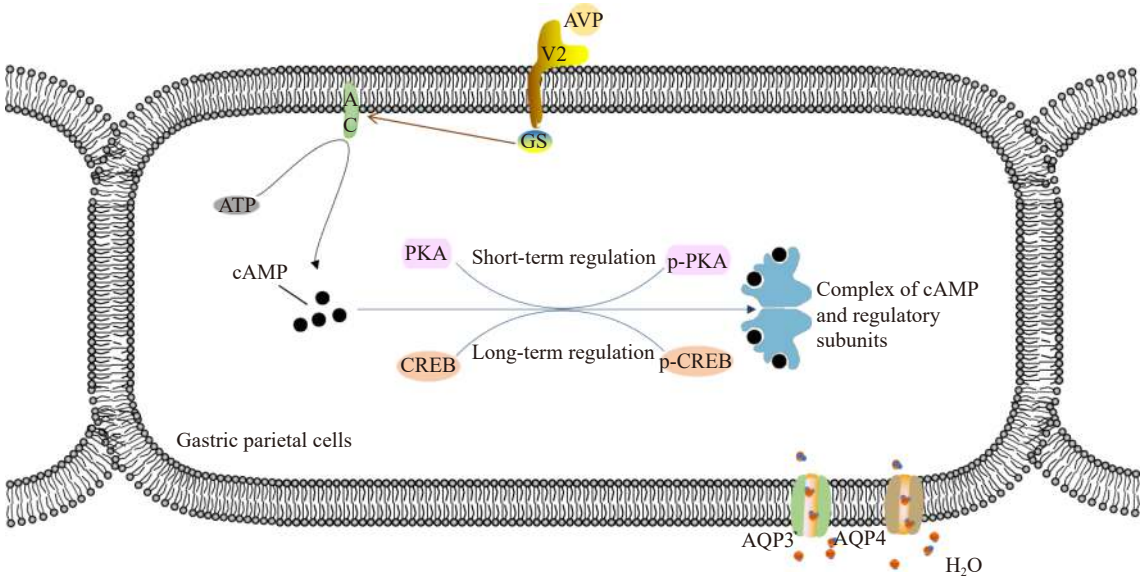

Fig. 11 Graph of proteins involved in the "AC-cAMP-AQP" signaling pathway

action of PWE on aquaporins, which further improves spleen function. Thus, the spleen has a healthy function and the dampness in the body is reduced. We intend to further explore the water metabolism signaling pathways in the small intestine and colon, which are involved in treating DSSD, to gain a more comprehensive understanding of the mechanism of Poria in treating DSSD.

Conclusions

PWE treatment leads to increases in fecal moisture percentage, urine output, D-xylose level, weight, swimming time, and AMS, ALB, and TP in rats. 16*α*-Hydroxydehydrotrametenolic acid, 16*α*-hydroxytrametenolic acid, polyporenic acid C, dehydrotumulosic acid, tumulosic acid, poricoic acid HE, 3-*epi*-dehydrotumulosic acid, 3-*O*-acetyl-16*α*-hydroxydehydrotrametenolic acid, 3-*O*-acetyl-16*α*-hydroxytrametenolic acid, dehydropachymic acid, and pachymic acid are determined to be the main effective components of Poria in treating DSSD for the first time. Regulation of the gastrointestinal hormones (MTL and GAS), "AC-cAMP" signaling pathway (ADH, ADCY5/6, PKA, p-PKA*α*/*β*/*γ* cat, CREB, p-CREB, AQP3, and AQP4), and gastrointestinal-related proteins (AQP1 and AQP3 in the duodenum; AQP3 and AQP4 in the colon) may be the mechanism of PWE in treating DSSD. Overall, our results suggest the multicomponent, multi-effect, and collaborative integration characteristics of PWE. These findings may provide new theoretical evidence for better application of Poria in the treatment of DSSD.

Supporting Information

Supporting information of this paper can be requested by sending E-mails to the corresponding authors.

References

[1] Zhao WX, Cui N, Jiang HQ, *et al*. Effects of Radix Astragali and its split components on gene expression profiles related to water metabolism in rats with the dampness stagnancy due to spleen deficiency syndrome [J]. *Evid Based Complement Alternat Med*, 2017, **2017**: 4946031.

[2] Zhang X, Li S, Ren Y, *et al*. Li Shengcai's experience in treating chronic gastritis of dampness obstructing middle Jiao type [J]. *China Natur*, 2021, **29**(2): 38-39.

[3] Verkman AS, Anderson MO, Papadopoulos MC. Aquaporins: important but elusive drug targets [J]. *Nat Rev Drug Discov*, 2014, **13**(4): 259-277.

[4] Wang L, Huang X, Yang C, *et al*. Distribution of the pathological features of AQP1 in gastrointestinal tissue of the animal model of the syndrome of dampness incumbering middle energizer [J]. *Lishizhen Med Mater Med Res*, 2011, **22**(9): 2279-2281.

[5] Shi K, Qu L, Lin X, *et al*. Deep-fried Atractylodis Rhizoma protects against spleen deficiency-induced diarrhea through regulating intestinal inflammatory response and gut microbiota [J]. *Int J Mol Sci*, 2019, **21**(1): 124.

[6] Kuwahara M, Fushimi K, Terada Y, *et al*. cAMP-dependent phosphorylation stimulates water permeability of aquaporin-collecting duct water channel protein expressed in *Xenopus oocytes* [J]. *J Biol Chem*, 1995, **270**(18): 10384-10387.

[7] Zheng Y, Zeng X, Chen P, *et al*. Integrating pharmacology and gut microbiota analysis to explore the mechanism of *Citri peticulatae* pericarpium against reserpine-induced spleen deficiency in rats [J]. *Front Pharmacol*, 2020, **11**: 586350.

[8] Lu A, Jia H, Xiao C, *et al*. Theory of traditional Chinese medicine and therapeutic method of diseases [J]. *World J of gastroentero*, 2004, **10**(13): 1854-1856.

[9] *National Pharmacopoeia Committee Chinese Pharmacopoeia*, Volume I [S]. Beijing: China Medical Science and Technology Press, 2020: 251.

[10] Jiang Y, Fan L. Evaluation of anticancer activities of *Poria cocos* ethanol extract in breast cancer: *in vivo* and *in vitro*, identification and mechanism [J]. *J Ethnopharmacol*, 2020, **257**: 112851.

[11] Peng W, Tan H, Zhan J, *et al*. Optimization of bioprocess extraction of *Poria cocos* polysaccharide (PCP) with aspergillus niger *β*-glucanase and the evaluation of PCP antioxidant property [J]. *Molecules*, 2020, **25**(24): 5930.

[12] Jeong J, Lee H, Han M, *et al*. Ethanol extract of *Poria cocos* re-

duces the production of inflammatory mediators by suppressing the NF-kappaB signaling pathway in lipopolysaccharide-stimulated RAW 264.7 macrophages [J]. *BMC Complement Altern Med*, 2014, **14**: 101.

[13] Zhao Y, Feng Y, Du X, *et al*. Diuretic activity of the ethanol and aqueous extracts of the surface layer of *Poria cocos* in rat [J]. *J Ethnopharmacol*, 2012, **144**(3): 775-778.

[14] Tian H, Liu Z, Pu Y, *et al*. Immunomodulatory effects exerted by *Poria cocos* polysaccharides *via* TLR4/TRAF6/NF-kappaB signaling *in vitro* and *in vivo* [J]. *Biomed Pharmacother*, 2019, **112**: 108709.

[15] Li H, Wang T, You P, *et al*. Clearing damp and promoting diuresis effect of *Poria cocos* from different origins on lower energizer edema of rat with kidney-yang deficiency [J]. *Tradit Chin Drug Res Clin Pharmacol*, 2021, **32**(5): 632-638.

[16] Yang T, Xu X, Dou D. Study on effect of *Poria cocos* on fluid retention of upper jiao in rats [J]. *Liaoning J Tradit Chin Med*, 2017, **44**(5): 1096-1099.

[17] Xia B, Zhou Y, Tan H, *et al*. Advanced ultra-performance liquid chromatography-photodiode array-quadrupole time-of-flight mass spectrometric methods for simultaneous screening and quantification of triterpenoids in *Poria cocos* [J]. *Food Chem*, 2014, **152**: 237-244.

[18] Zhang Y, Wu M, Xi J, *et al*. Multiple-fingerprint analysis of *Poria cocos* polysaccharide by HPLC combined with chemometrics methods [J]. *J Pharm Biomed Anal*, 2021, **19**(10): 114012.

[19] Li R, Yan Z, Li W, *et al*. Establishing spectrum effect relationship of traditional Chinese medicine [J]. *Educ Chin Med*, 2002, **21**(2): 62.

[20] Feng Y, Teng L, Wang Y, *et al*. Using spectrum-effect relationships coupled with LC-TOF-MS to screen anti-arrhythmic components of the total flavonoids in *Hypericum attenuatum* extracts [J]. *J Chromatogr Sci*, 2021, **59**(3): 246-261.

[21] Qiao R, Zhou L, Zhong M. Spectrum-effect relationship between UHPLC-Q-TOFMS fingerprint and promoting gastrointestinal motility activity of Fructus Aurantii based on multivariate statistical analysis [J]. *J Ethnopharmacol*, 2021, **279**(28): 114366.

[22] Tu Y, Luo X, Liu D, *et al*. Extracts of *Poria cocos* improve functional dyspepsia *via* regulating brain-gut peptides immunity and repairing of gastrointestinal mucosa [J]. *Phytomedicine*, 2022, **95**: 153875.

[23] Wang T, Li H, Zhang D, *et al*. Establishment of UPLC fingerprint of *Poria cocos* aqueous extract and study on its spectrum-effect relationship with sedative and hypnotic effect [J]. *Chin Pharm*, 2021, **32**(5): 564-570.

[24] Fu W, Sun X, Sun S, *et al*. Effects of Atractylodis Rhizoma before and after being deep-flied on contents of aquaporin 2 and aquaporin 3 in model rats with syndrome of damp retention in middle-jiao [J]. *Chin J Exp Tradit Med Formu*, 2016, **22**(9): 19-22.

[25] Xue X, Huang X, Gao N, *et al*. Effects of Huoxiang Zhengqi liquid on the expression of AQP4 in colon mucosa in rats with dampness retention syndrome [J]. *Chin J Exp Tradit Med Formu*, 2012, **18**(19): 165-169.

[26] Feng G, Zheng Y, Sun Y, *et al*. A targeted strategy for analyzing untargeted mass spectral data to identify lanostane-type triterpene acids in *Poria cocos* by integrating a scientific information system and liquid chromatography-tandem mass spectrometry combined with ion mobility spectrometry [J]. *Anal Chim Acta*, 2018, **1033**: 87-99.

[27] Zhang D, Fan L, Yang N, *et al*. Discovering the main "reinforce kidney to strengthening yang" active components of salt *Morinda officinalis* based on the spectrum-effect relationship combined with chemometric methods [J]. *J Pharm Biomed Anal*, 2022, **207**: 114422.

[28] Cai H, Li H, Zeng H, *et al*. Application evaluation of clinical practice guidelines for traditional Chinese medicine: a clinical analysis based on the analytic hierarchy process [J]. *BMC Complement Med*, 2019, **19**(1): 277.

[29] Xu J. Effect of Shenling Baizhu powder on digestive and absorptive function of rats with diarrhea due to spleen deficiency [J]. *Acta Chin Med*, 2020, **261**(35): 366-369.

[30] Lu Y, Li Q, Zhan H, *et al*. Clinical effect of acupoint patching combined with massage for functional constipation in children syndrome of spleen deficiency and liver hyperactivity [J]. *J Hebei Tradit Chin Med Pharmacol*, 2022, **44**(4): 651-655.

[31] Niu Y. The shallows of Shenling Baizhu powder in applying of treating spleen-deficiency constipation [J]. *World Latest Med Inform*, 2019, **19**(28): 236-238.

[32] Shen H, Zhao Q, Yan H. Clinical study on the treatment of children functional constipation of spleen deficiency and intestinedryness type by Shengjiang Runchang formula [J]. *Beijing J Tradit Chin Med*, 2022, **44**(4): 370-373.

[33] Li X, Qiu W, Da X, *et al*. A combination of depression and liver Qi stagnation and spleen deficiency syndrome using a rat model [J]. *Anat Rec (Hoboken)*, 2020, **303**(8): 2154-2167.

[34] Mei L, Wang F, Yang M, *et al*. Studies on the mechanism of the volatile oils from Caoguo-4 decoction in regulating spleen deficiency diarrhea by adjusting intestinal microbiota [J]. *Oxid Med Cell Longev*, 2022, **2022**: 5559151.

[35] Li B, Hou W, Wang C, *et al*. Study on the characteristics of water metabolism in spleen deficiency animals [J]. *Liaoning J Tradit Chin Med*, 2016, **43**(1): 150-153.

[36] Li L, Zuo Z, Wang Y. Practical qualitative evaluation and screening of potential biomarkers for different parts of *Wolfiporia cocos* using machine learning and network pharmacology [J]. *Front Microbiol*, 2022, **13**: 931967.

[37] Xu H, Wang Y, Jurutka P, *et al*. 16α-Hydroxytrametenolic acid from *Poria cocos* improves intestinal barrier function through the glucocorticoid receptor-mediated PI3K/Akt/NF-kappaB pathway [J]. *J Agric Food Chem*, 2019, **67**(39): 10871-10879.

[38] Zhou L, Zhang Y, Apter L, *et al*. Cytotoxic and anti-oxidant activities of lanostane-type triterpenes isolated from *Poria cocos* [J]. *Chem Pharm Bull (Tokyo)*, 2008, **56**(10): 1459-1462.

[39] Li T, Hou C, Chang C, *et al*. Anti-hyperglycemic properties of crude extract and triterpenes from *Poria cocos* [J]. *Evid Based Complement Alternat Med*, 2011, **2011**: 128402.

[40] Ukiya M, Akihisa T, Tokuda H, *et al*. Inhibition of tumor-promoting effects by poricoic acids G and H and other lanostane-type triterpenes and cytotoxic activity of poricoic acids A and G from *Poria cocos* [J]. *J Nat Prod*, 2002, **65**(4): 462-465.

[41] Lee SR, Lee S, Moon E, *et al*. Bioactivity-guided isolation of anti- inflammatory triterpenoids from the sclerotia of *Poria cocos* using LPS-stimulated Raw264.7 cells [J]. *Bioorg Chem*, 2017, **70**: 94-99.

[42] Feng G. *Study on the material basis of Ding-Zhi-Xiao-Wan prescription in the treatment of Alzheimer's disease in vitro and in vivo based on mass spectrometry* [D]. University of Science and Technology of China, 2019.

[43] Tu J, Xie Y, Xu K, *et al*. Treatment of spleen-deficiency syndrome with atractyloside a from bran-processed atractylodes lancea by protection of the intestinal mucosal barrier [J]. *Front Pharmacol*, 2020, **11**: 583160.

[44] Ma T, Verkman A. Aquaporin water channels in gastrointestinal physiology [J]. *J Physiol*, 1999, **517**(2): 317-326.

[45] Peng Y, Zhang C, Su Y, *et al*. Activation of the hippocampal AC-cAMP-PKA-CREB-BDNF signaling pathway using WTKYR in depression model rats [J]. *Electrophoresis*, 2019,

40: 1245-1250.
[46] Zhang H, Chen J, Huang X. Influence of Pingwei San on AC-cAMP-PKA pathway in gastric mucosa of rats with syndrome of accumulation of dampness in middle-jiao [J]. *Lishizhen Med Mater Med Res*, 2013, **24**(12): 2829-2831.
[47] Masyuk A, Marinelli R, LaRusso N. Water transport by epithelia of the digestive tract [J]. *Gastroenterology*, 2002, **122**(2): 545-562.
[48] Powell D. Barrier function of epithelia [J]. *Am J Physiol*, 1981, **241**(4): 275-288.
[49] Yue X. *Effect and mechanism of Danggui-Shaoyao-San on nephrotic syndrome based on the path of AVP-V2R-AQP2* [D]. Journal of Anhui Traditional Chinese Medical College, 2015.
[50] Ikarashi N, Nagoya C, Kon R, *et al*. Changes in the expression of aquaporin-3 in the gastrointestinal tract affect drug absorption [J]. *Int J Mol Sci*, 2019, **20**(7): 1559.
[51] Ikarashi N, Ushiki T, Mochizuki T, *et al*. Effects of magnesium sulphate administration on aquaporin 3 in rat gastrointestinal tract [J]. *Biol Pharm Bull*, 2011, **34**(2): 238-242.

Cite this article as: LI Huijun, ZHANG Dandan, WANG Tianhe, LUO Xinyao, XIA Heyuan, PAN Xiang, HAN Sijie, YOU Pengtao, WEI Qiong, LIU Dan, ZOU Zhongmei, YE Xiaochuan. Screening the effective components in treating dampness stagnancy due to spleen deficiency syndrome and elucidating the potential mechanism of Poria water extract [J]. *Chin J Nat Med*, 2023, **21**(2): 83-98.

YE Xiaochuan, Ph.D., is the professor and doctoral supervisor of the School of Pharmacy, Hubei University of Traditional Chinese Medicine. She also works as the Executive Deputy Director of the Hubei Key Laboratory of Resources and Chemistry of Chinese Medicine. More than 20 sub-projects of the National Key Research and Development Plans, the National Natural Science Foundations, the Provincial Department-level Projects, and the Horizontal Projects have been presided. Prof. YE has published about 90 academic papers (more than 10 SCI included), and she has owed 9 authorized patents. Her main research interests are: (1) Study on the basis of pharmacodynamic substances and quality control of traditional Chinese medicine; (2) Research and development of new TCM products.

ZOU Zhongmei is the professor, doctoral supervisor and the director of the Center for Natural Medicine Chemistry, Institute of Medicinal Plants, Chinese Academy of Medical Sciences. She also serves as the visiting professor of the “Lakeside Scholars Program” at Hubei University of Chinese Medicine. To date, more than 20 National Science and Technology Key Projects, “Major New Drug Creation” and the National Natural Science Foundation Projects were in charge. She undertook and established the “National TCM Compound Library” for the large-scale preservation of TCM chemical components. More than 300 academic papers were published, including 160 SCI papers, and 10 patents have been obtained. Prof. ZOU leads a research group focusing on the material basis and mechanism of traditional Chinese medicine and its compounds based on metabonomics.